Geophys. J. Int. (1998) **134,** 409–421

Temporal and three-dimensional spatial analyses of the frequency–magnitude distribution near Long Valley Caldera, California

Stefan Wiemer,[1] Stephen R. McNutt[2] and Max Wyss[2]

[1] *Seismology and Volcanology Research Department, Meteorological Res. Inst., Nagamine, Tsukuba* 305*, Japan. E-mail: stefan@mri-jma.go.jp*
[2] *Geophysical Institute, University of Alaska Fairbanks, Fairbanks,* AK 99775–7320*, USA. E-mail: steve@giseis.alaska.edu,max@giseis.alaska.edu*

Accepted 1998 February 16. Received 1998 February 12; in original form 1997 December 3

SUMMARY

The 3-D distribution of the *b* value of the frequency–magnitude distribution is analysed in the seismically active parts of the crust near Long Valley Caldera, California. The seismicity is sampled in spherical volumes, containing $N = 150$ earthquakes and centred at nodes of a grid separated by 0.3 km. Significant variations in the *b* value are detected, with *b* ranging from $b \approx 0.6$ to $b \approx 2.0$. High *b*-value volumes are located near the resurgent dome, and at depths below 5 km at Mammoth Mountain. *b* values are found to be much lower south of the Long Valley Caldera. We interpret this to indicate that an active magma body has advanced from depths below 8 km to depths of 4 to 5 km beneath Mammoth Mountain in 1989, and that anomalous crust, either highly fractured or containing unusually high pore pressure, such as is the case in the vicinity of active magma bodies, exists north of the seismically active area beneath the resurgent dome at all depths. We also investigate the spatial distribution of temporal variations of the frequency–magnitude distribution by introducing differential *b*-value maps. *b* values increased from $b \approx 0.8$ to $b \approx 1.5$ underneath Mammoth Mountain at the onset of the 1989 earthquake swarm and remained high thereafter. This suggests that an intrusion permanently altered the average distribution of cracks at 5–10 km depth, or that the pore pressure permanently increased. We propose that high *b* values are a necessary (but not sufficient) condition near a magmatic body, and therefore spatial *b*-value mapping can be used to aid in the identification of active magma bodies.

Key words: *b* value, Long Valley California, volcanic structure.

INTRODUCTION

The Long Valley Caldera in California is a tectonically complex and important region. Many geophysical studies have been performed in it (e.g. Bailey & Hill 1990; Shih & Meyer 1990; Langbein *et al.* 1993; Sorey *et al.* 1993; Pitt & Hill 1994; Weiland *et al.* 1995), giving us a solid understanding of the region's tectonic framework and geological history. The formation of the caldera and the most recent eruptions in or adjacent to the caldera took place about 700 000 and 50 000 years ago, respectively. The Mono and Inyo craters to the north of the caldera erupted about 600 years ago (Miller 1985; Sieh & Bursik 1986). The resurgent dome within the caldera has inflated at a rate of about 2–3 cm per year since 1989 (Langbein *et al.* 1993; Dixon *et al.* 1997). Major episodes of seismic activity from 1980 to 1989 (Table 1) have heightened the awareness that Long Valley Caldera remains a tectonically active region.

In this paper, we map the *b* value of the frequency–magnitude distribution (FMD) in the Long Valley area. Thanks to the rich data set of earthquakes located during the past 15 years, 3-D mapping can be performed with a resolution of less than 0.5 km. The *b* value has been the subject of many studies in the past decades, and the information contained in the FMD was widely assumed to have been exhausted. However, recently we have applied a dense gridding approach to mapping *b* in detail using high-quality regional earthquake catalogues (Wiemer & Benoit 1996; Wiemer & Wyss 1997; Wyss *et al.* 1997; Wiemer & Katsumata 1998). In all tectonic regimes investigated, we found statistically highly significant spatial variations in the FMD over distances of one to several kilometres.

Studies in volcanic regions have been especially fruitful in mapping crustal volumes with different mean magnitudes, because here the contrast between the 'normal' tectonic crust and anomalously high *b*-value regions is especially striking.

Date		Event
May 25-27,	1980	Four M6 Mammoth Lakes earthquakes
Sept 30,	1981	M5.9 Laurel Mountain earthquake 10 km S of LVC
mid-May	1982	USGS seismic network installed - high quality data starts
Jan 7,	1983	Two M5.3 South Moat earthquakes inside LVC
July	1984	last M4 inside caldera, strain rate decreasing
Nov 23,	1984	M6.1 Round Valley earthquake 20 km SE of LVC
July 21,	1986	M6.4 Chalfant earthquake 30 km east of LVC caused ~10 cm strain step in deformation
May-Oct	1989	Mammoth Mountain swarm
Oct 23,	1990	M5.7 Mono Lake earthquake 25 km N of LVC
fall	1989	strain rate increases in LVC, leads seismicity by about 2 months
June 28,	1992	Landers M7.5 earthquake triggers seismicity rate increase
June	1997	Increased seismic activity near the resurgent dome, possibly due to pressure increase in main magma chamber at depth.

The first study of this kind was performed by Wiemer & McNutt (1997) and targeted the seismicity underneath Mount St Helens (Washington) and Mt Spurr (Alaska). The authors point out a correlation between a region of anomalously high b value and the main magma chamber believed to be at a depth of about 6–7 km underneath the summit of Mount St Helens. A second high b-value anomaly at a depth of about 3–4 km underneath the summit was found in a depth range where violent vesiculation is believed to have occurred during the 1980 eruption. The third volcanic system studied in detail using spatial b-value mapping was the Off-Ito eruption off the Izu coast in Central Japan (Wyss *et al.* 1997). A high b-value anomaly with 2 km radius was detected at a depth below 7 km underneath and somewhat southwest of the Off-Ito volcano. The hypothesis that this small volume of high b values is indicative of a nearby active magma chamber is in good agreement with observations from geodetic deformation measurements, which indicate that erupting magma worked its way up from a depth below 7 km through a narrow dike in the top of the crust. Common to Mount St Helens and Off-Ito was the finding that pockets of high b value ($b > 1.3$) are embedded in an average tectonic crust ($b < 1$), which is a refinement to the commonly held simplistic view that volcanic systems are characterized by high b values.

The frequency–magnitude distribution (Ishimoto & Iida 1939; Gutenberg & Richter 1944) describes the power-law relationship between the frequency of occurrence and magnitude of earthquakes:

$$\log_{10} N = a - bM, \quad (1)$$

where N is the cumulative number of earthquakes having magnitudes larger than M, and a and b are constants. The original formulation by Ishimoto & Iida (1939) as well as that by Gutenberg & Richter (1944) used the absolute rather than the cumulative frequency of earthquakes. However, from a practical and statistical standpoint it is preferable to use the cumulative frequency–magnitude distribution. Various methods have been suggested to measure b and its confidence limits (Shi & Bolt 1982). The b value has been shown to be scale-invariant down to a source length of about 10 m (Abercrombie & Brune 1994; Abercrombie 1995).

Several factors can cause perturbations of the normal b value: increased material heterogeneity results in high b values (Mogi 1962); an increase in applied shear stress (Scholz 1968; Urbancic *et al.* 1992), or an increase in effective stress (Wyss 1973), decreases the b value. In addition, an increase in the thermal gradient causes an increase in b (Warren & Latham 1970). Thus, it may not always be clear which of these factors causes an observed b-value anomaly, unless other clues are available. Therefore, we seek to compare b-value anomalies to other known parameters of the crust, with the aim of obtaining evidence for the cause of the anomaly. b values measure differences in average crack size. Since the b value is inversely proportional to the mean magnitude (Aki 1965; Utsu 1965; Hamilton 1967), low b values indicate that the average crack length (or fault segment) that ruptures in an earthquake is larger in that volume than in a volume characterized by high b values. Because much evidence shows that the Earth's crust is strongly heterogeneous on scales of 1–10 km, we must expect that local differences in stress and material should lead to differences in the distribution of crack size. Hence, by mapping b values on a subkilometre scale, we may be able to map the variations of local crustal conditions.

Long Valley has been an especially rich source of earthquakes over the last two decades. In addition to the major events shown in Table 1, tens of thousands of smaller events have been located, and inflation of more than 0.6 m has been measured since 1975 (Dvorak & Dzurisin 1997). Intrusion of magma is thought to have caused a strong earthquake swarm in the south moat of the caldera in January 1983 (Rundle & Whitcomb 1984) and another one in 1989 beneath Mammoth Mountain (Hill *et al.* 1990; Cramer & McNutt 1997). The rate of horizontal deformation declined gradually from 1984 to 1989 (Langbein *et al.* 1993). At the time of the Chalfant Valley earthquake in July 1986, the caldera was subjected to a strain step of approximately 10 cm (Gross & Savage 1987). Later, seismicity increased abruptly at the time of the Landers earthquake in June 1992 (Hill *et al.* 1995). Thus, over the period of our study, significant changes in stress have occurred as well as intrusion of magma with accompanying heat and fluid exsolution. These factors make Long Valley an ideal place

to perform a study of changes in b, both temporally and spatially.

Many studies have presented geophysical evidence for the existence of large-scale bodies of magma in Long Valley. The most prominent anomalies overlap each other and are centred beneath the south and northwest portions of the resurgent dome (Rundle *et al.* 1986). A recent study by Weiland *et al.* (1995) shows a 25–30 per cent low-velocity zone centred at a depth of 11.5 km beneath the northwestern quadrant of the caldera. Although methods have evolved and the dimensions and magnitudes have varied, the anomalies have been spatially persistent for over 20 years.

In this paper, we test the hypothesis that the average crack distribution, or b value, is anomalous in the vicinity of active magmatic systems by mapping the frequency–magnitude distribution in the Long Valley area in three dimensions. We also refine our analysis techniques by introducing differential b-value maps, which identify volumes of significant temporal changes in the mean magnitude.

DATA

The data used in this study were provided by the Northern California Earthquake Data Centre (NCEDC), which processes events recorded by the Northern California Seismic Network operated by the US Geological Survey in Menlo Park. High-quality earthquake monitoring in the Long Valley region started in about May 1982 with magnitude of completeness (M_c) levels around 1.1–1.3. Fig. 1 shows an epicentre map of the Long Valley Caldera region. The two regions that we investigate in this study are the area underneath Mammoth Mountain, where an intense seismic swarm, lasting 6 months, was observed in 1989; and the seismicity along the southern rim of the Caldera and to the south.

Our analysis starts with the Mammoth Mountain area because the 1989 swarm observed at this location (Hill *et al.* 1990) provides a rich source of information and the intrusion that probably caused the swarm is an important tectonic event. An earlier period of unrest at Long Valley Caldera, from 1980 to 1982, was recorded only with an inferior seismic network and is therefore not investigated in this study.

METHOD

3-D analysis of the FMD

To calculate a b value, a sample of size N is selected, where either N or the sample volume is kept constant. We prefer a constant number of events in each sample to ensure that a change in the sample size does not affect the analysis. However, the shape of the sampling volume is a free parameter. In the past, we have performed the analysis of the b value using either b-value maps (Wyss *et al.* 1997) or cross-sectional views (Wiemer & Benoit 1996; Wiemer & McNutt 1997; Wiemer & Wyss 1997). In both of these cases, the sampling volumes are cylinders, which may have an axis longer than the radius. In

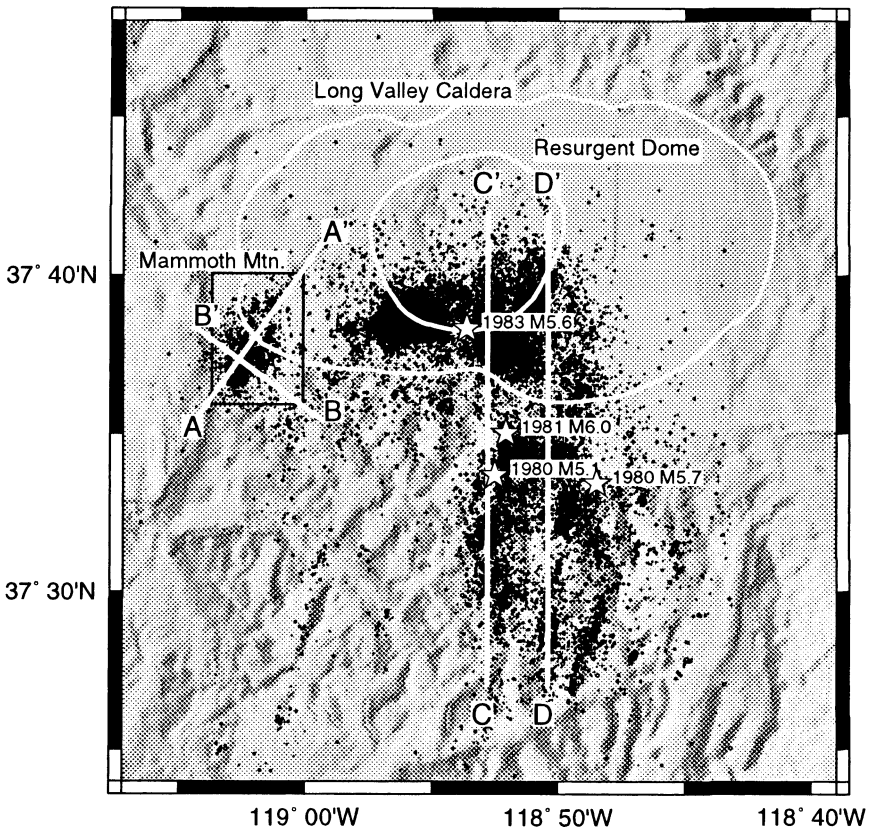

Figure 1. Epicentre map of the area near Long Valley Caldera. Epicentres from 1983 to 1997.8 are shown as dots, scaled proportional to magnitude. Stars indicate the location of $M = 5$ events. The outlines of the caldera and the resurgent dome are shown. The positions and orientations of four cross-sections (A–D) used in Figs 4, 6, and 7 are indicated.

this paper, we map the FMD in three dimensions using spherical volumes. Ogata *et al.* (1991) perform a three dimensional analysis of the b value in the Kanto area, Japan, by using a maximum-likelihood criterion rather than a fixed sample size. In our analysis, a 3-D grid (lat, lon, z) is created with a typical grid spacing of 0.3 km. We sample the N nearest neighbours around each grid point in a Euclidean sense for estimating b. N is constant and usually in the range of 100–500; thus, the radius of each sphere is inversely proportional to the local density of earthquakes. Because we choose dense grid spacing, the spheres overlap. The b value estimated for each volume is represented by a colour code at each node. The images obtained are smoothed using a spline interpolation.

During the analysis, anomalies are interactively confirmed by inspecting the appearance of the FMD and the quality of the straight-line fit. We specifically search for volumes displaying a bi-modal FMD, because a Gutenberg–Richter type power law cannot adequately describe this behaviour and therefore volumes that may show this behaviour should be excluded from the analysis. There are two advantages to a true 3-D analysis over the 2-D analysis: (1) a 3-D grid is independent of the particular cross-sectional view chosen by the analysts; and (2) spherical volumes avoid oddly shaped sample volumes such as extremely elongated cylinders. The 3-D matrix of b values, b(lat, lon, z), can be viewed along any surface. To check the results presented below, we compared them with the analysis of vertical cross-sections and map views and found no significant differences.

We apply a standard moving-window technique to analyse the b value as a function of depth or time. Each window contains a constant number of events (typically 150 or 200) and the window is moved forward by a constant number of earthquakes (e.g. 15). For a more detailed discussion of the spatial mapping of the b value, we refer to Wiemer & Benoit (1996) and Wiemer & Wyss (1997).

The b value is calculated by the maximum-likelihood method. For each sample, the minimum magnitude of completeness, M_c, is estimated separately by taking the maximum value of the derivative of the frequency–magnitude distribution. This is done for each sample, because M_c can vary as a function of depth and location. Although the estimate of M_c by algorithm is fairly reliable, as judged by inspection, it can fail if magnitudes much smaller than M_c are included. Therefore, as a precaution we use only the data for $M > M_c$ as estimated for the entire data set. M_c for Long Valley is 1.3.

An estimate of the standard deviation, δb, of the b value can be obtained using the equation first derived by Aki (1965), or the improved formulation by Shi & Bolt (1982):

$$\delta b = 2.3 b^2 \sqrt{\frac{\sum_i (M_i - \langle M \rangle)}{n(n-1)}}, \qquad (2)$$

where n is the sample size. We estimate the probability that two samples may come from the same population by Utsu's (1992) test:

$$P \approx \exp(-\mathrm{d}A/2 - 2), \qquad (3)$$

where $\mathrm{d}A = -2N\ln N + 2N_1 \ln(N_1 + N_2 b_1/b_2) + 2N_2 \ln(N_1 b_2/b_1 + N_2) - 2$ and $N = N_1 + N_2$. This test accounts explicitly for the number of earthquakes contained in each sample. By using small samples to map b, one gains spatial resolution, but is penalised with lower probabilities that mapped anomalies are significant.

Differential *b*-value maps

We believe that changes in the frequency–magnitude distribution as a function of time are generally more difficult to evaluate than spatial variations for two reasons. (1) Network configuration modifications and analysing procedures are likely to change as a function of time and can introduce artefacts in the magnitudes reported (Habermann 1987; Habermann 1991; Wyss 1991). These changes in the reporting history can introduce artificial changes in the b values, for example a stretch in the FMD (Zuniga & Wyss 1995). (2) Temporal variations are usually second-order phenomena, rather than the first-order variations of the b value with location (Wiemer & Wyss 1997; Wiemer & Katsumata 1998). We have interpreted this as a sign that the production of earthquakes in a particular volume depends on stationary properties such as the crack distribution, and that a particular volume does not readily change its earthquake size distribution (Wiemer & Wyss 1997). However, in volcanic systems and during large earthquakes, dramatic changes in the crust do occur, for example the intrusion of a major dike or a change in pore pressure. It is therefore important to be able to study the temporal variations of a crustal volume reliably.

Temporal changes of b values can be mapped by 'differential b-value maps' in the following fashion. (1) Calculate a b-value grid for the period T_1–T_2, as described above, but using volumes of constant size. (2) Calculate a b-value grid for the period T_3–T_4, using the nodes defined in (1). (3) Compare the FMDs at each node for the two periods. (4) Plot the difference, using a colour code, if it is statistically significant at the 99 per cent confidence level as measured by Utsu's test (eq. 3). These differential b-value maps thus identify volumes of *significantly* increased or decreased b value.

RESULTS

The 1989 Mammoth Mountain intrusion

The b values in the 1989 Mammoth Mountain intrusion area show an increase from $b \approx 0.8 \pm 0.03$ to $b \approx 1.3 \pm 0.08$ at the time of the 1989 earthquake swarm (Fig. 2a). The results in Fig. 2(a) are based on $M_c = 1.3$, although we estimate the magnitude of completeness to be $M_c = 1.1$, or even lower for some periods in 1989 due to the addition of seismic stations. The increase in b by $+0.5$ appears to be permanent; b remains high until the end of the period investigated (1997.7). The difference in the two populations can be established as statistically highly significant, based on the test by Utsu. The frequency–magnitude distributions follow a Gutenberg–Richter power-law model closely; no indication of a bi-modal FMD can be seen in the data.

The dependence of the b value on depth in the bulk data set below the Mammoth Mountain area is shown in Fig. 2(b). To minimize the influence of temporal changes we use only data from the main intrusion period (1989.5–1990.5). The moving window to calculate b contains 150 earthquakes and is stepped by 15 events. The b value decreases gradually from about $b = 1.15 \pm 0.04$ at the surface to its minimal value of 1.0 at a depth of 4 km, below which it rises sharply to a peak of

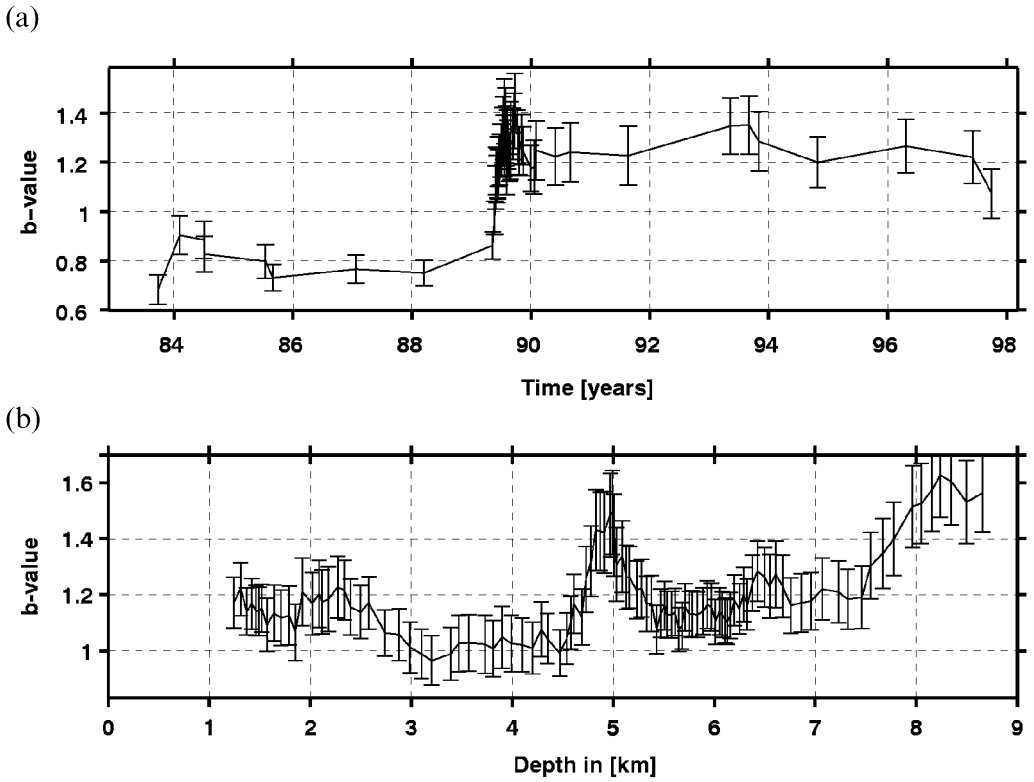

Figure 2. Seismicity in the Mammoth Mountain area. (a) b value as a function of time. (b) b value as a function of depth for the period 1989–1990.5. In both figures, each sliding time window contains 150 events.

$b = 1.3 \pm 0.05$ at 5 km depth. At greater depths, the b values are at first somewhat lower ($b \approx 1.2$) than at 5 km depth, but then increase to their maximum of $b \approx 1.4 \pm 0.06$ at 8 km depth.

The 3-D image of the b-value distribution below the Mammoth Mountain area is based on a grid with spacing $0.3 \times 0.3 \times 0.3$ km and sampling by the $N = 150$ closest earthquakes to each node (Fig. 3). The b values are presented in a colour code in selected planes of interest that convey a maximum amount of information, without cluttering the picture. The average sampling radius of the spheres is $r = 1$ km, and nodes are coloured only if the radius is less than $r = 1.5$ km; otherwise we consider the volumes sampled to be too large to describe the local seismicity adequately.

Most of the crustal volume below Mammoth Mountain shows normal to slightly elevated b values in the range of 0.9–1.2 (blue colours in Fig. 3). The highest b values, of 1.8 ± 0.07, are detected at depths of 8–9 km in a volume with $r = 1$ km at the bottom of the seismogenic zone. In addition, a smaller volume ($r = 0.5$ km) with $b = 1.5 \pm 0.06$ exists between 4 and 5 km depth at the core of the seismicity. This coincides with the depth of mixed-frequency events as described by Cramer & McNutt (1997).

The two vertical cross-sections, along and perpendicular to the strike of the intruded dike as inferred by Hill *et al.* (1990) (Fig. 4), confirm the results shown in Figs 2 and 3: most volumes at shallow depths show normal b values; a major anomaly of very high b values exists at depths below 7 km; and a small volume of high b values is seen at 5 km depth. In addition, the small anomaly ($r = 0.3$ km) of high b values at 1.3 km depth, also seen in Fig. 3, is brought out more clearly in Fig. 4(b). The comparison of FMDs for two volumes, one shallow, one deep, shows that the differences are statistically highly significant (Fig. 5a). The shallow volume has a b value of 0.93 ± 0.04, the deep volume one of 1.73 ± 0.06.

The temporal b-value change, documented in Fig. 2, is mapped in the differential b-value cross-section of Fig. 6, which compares the periods 1983–89 and 1989–97. The radii of the volumes investigated were constant ($r = 2$ km). At each node, we determine if the difference in b is significant at the 99 per cent confidence level; at nodes that fail this test, the b value is considered unchanged. Fig. 6 shows that we observe an increase in b at many nodes for the later period. This increase can be as large as $+0.65$, and is most pronounced at greater depths. None of the nodes shows a decrease in b value. For a selected node, we show the two magnitude–frequency distributions (Fig. 5b) where we observe an increase of b from $b = 0.79 \pm 0.04$ to $b = 1.36 \pm 0.05$. In most of the volumes, we also observe an increase in the parameter 'a' that describes the productivity of each volume (e.g. Fig. 5b).

Seismicity southeast of the resurgent dome

The bulk of the seismicity in the Long Valley area is located south and southeast of the resurgent dome (Fig. 1). Two clusters of seismicity can be distinguished on the southern edge of the caldera. These clusters have been active for the duration of the seismic monitoring, with significant fluctuations in the rate of earthquakes produced. Several main shocks with magnitudes above $M = 5$ have occurred here since 1980 (Table 1), each producing pronounced aftershock sequences. A clear increase in activity took place around 1989.4, coinciding with the Mammoth Mountain swarm. We restrict our analysis to

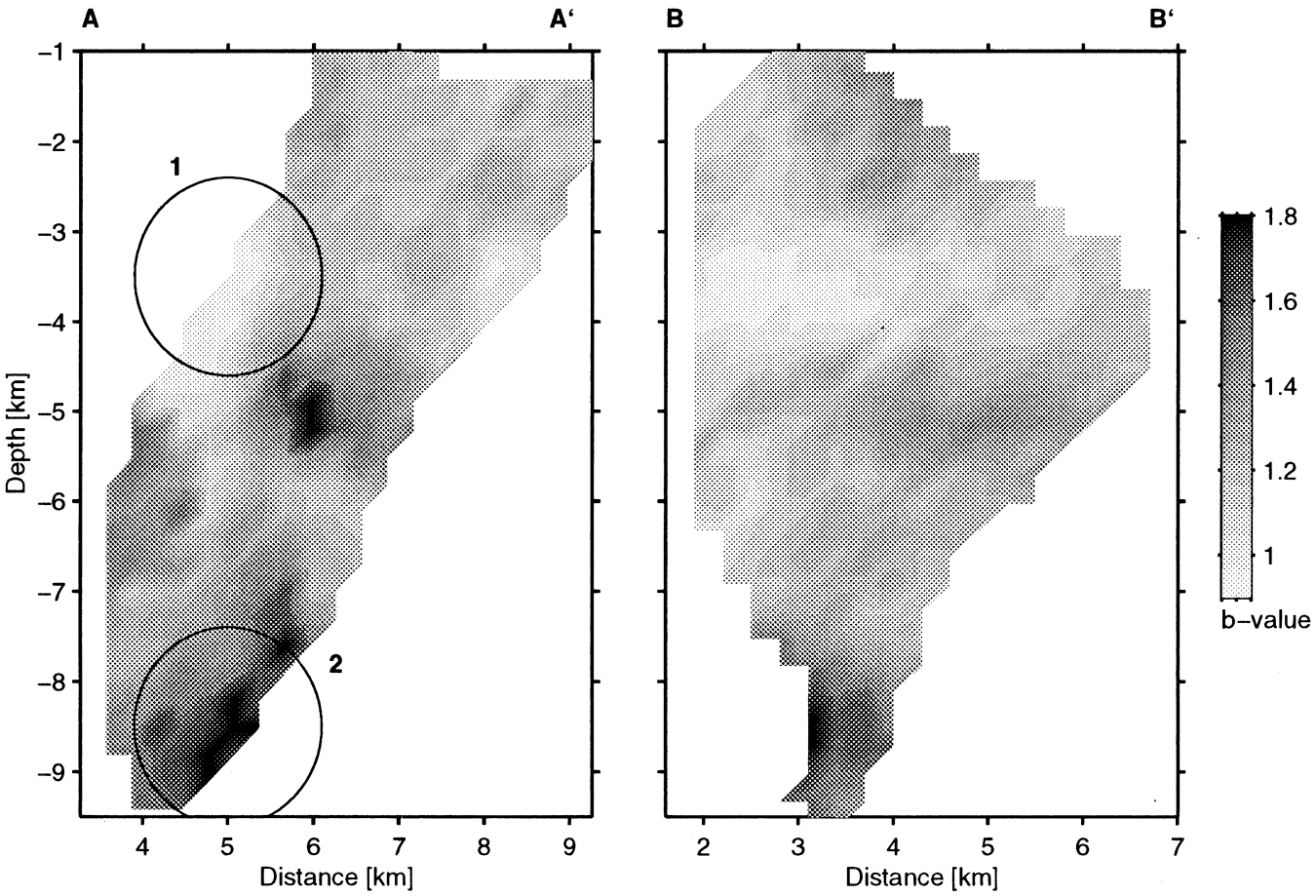

Figure 4. Cross-sections of b values (a) along and (b) perpendicular to the dike intruded in 1989 under Mammoth Mountain (see Fig. 1 for definition). The spacing of the grid was 0.3 km and the $N=150$ nearest earthquakes were used. Dark colours identify volumes of high b values. The two circles indicate volumes compared in Fig. 5(a).

the period 1989.0–1997.8, because the more recent data are more complete and homogeneous in magnitude reporting, and no major aftershock sequence exists in this period.

For the Long Valley area, we also compute a 3-D matrix of the b values using sampling spheres containing 150 earthquakes each. Two vertical, NS-striking cross-sections along profiles C–C′ and D–D′ (Fig. 1) through the matrix of b values are shown in Fig. 7. In both of these cross-sections we find the highest b values ($b \approx 1.8 \pm 0.1$) at the northernmost end. Most of the volumes show low to normal values (0.6–1.1), with the lowest b values in the south and at depth. In addition, we observe a general decrease of b with depth for the seismicity everywhere, except in the northern, anomalous volume. Figs 5(c,d) compare the frequency–magnitude distribution for four selected volumes that are marked in the cross-sections of Fig. 7.

In six map views through the matrix of b values at depths of 1, 3, 5, 7, 9, and 11 km, the highest b values can be found in the northernmost part of the maps (Fig. 8). For all depths, except 7 km, high b values are contained within the resurgent dome area. At shallow depths (1–7 km), high b values are located in the southeastern quadrant of the resurgent dome, whereas for greater depths of 9 and 11 km we observe high b values throughout the seismically active part of the resurgent dome area. High b values of $b > 1.5$ are also observed underneath Mammoth Mountain at depths of 9 and 11 km.

In Fig. 9, we compare the depth gradient of the b value for the northernmost part of the seismicity, where high b values are found, with that of the 'normal' seismicity to the south. The overall frequency–magnitude distributions for the two volumes are shown in Fig. 5(d). As a function of depth, we find that the b values are similar to a depth of about 4 km (Fig. 9). At greater depths, however, opposite trends are observed. In the southern volume, the b values decrease with depth to a minimum of $b \approx 0.7$ at 10 km depth. In the northernmost volume they increase with depth to a maximum value of $b \approx 2.0$.

DISCUSSION

Significant spatial and temporal variations of the b value are detected by detailed analyses of the frequency–magnitude distribution of the seismicity in the Long Valley Caldera region. The highest b values are located near the active volcanic system, nearest to the resurgent dome (Figs 7 and 8) and in the close vicinity of the intruded dike in the Mammoth Mountain area (Figs 3 and 4). This supports the hypothesis of Wiemer & McNutt (1997) and Wyss *et al.* (1997), who

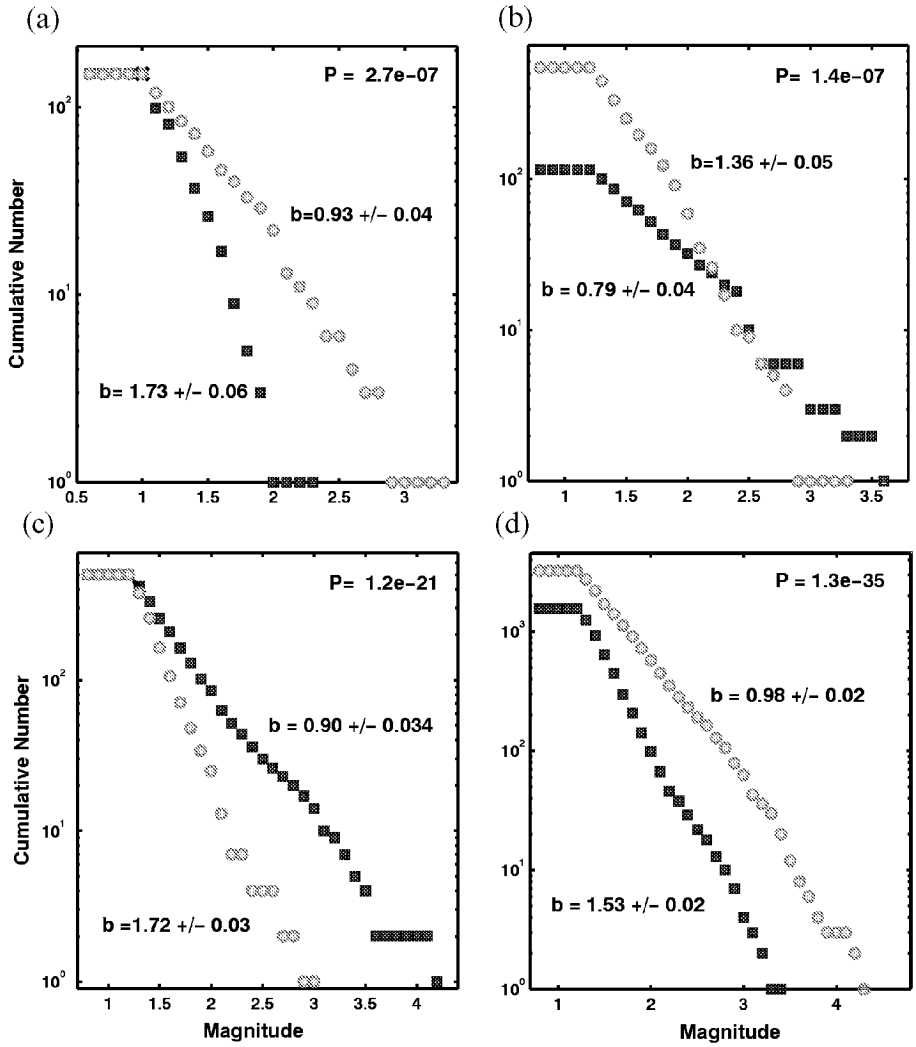

Figure 5. Examples of frequency–magnitude distributions. The volumes sampled are marked in (a) Fig. 4, (b) Fig. 6, (c and d) Fig. 7. The parameter *P* in the upper right corner of each graph is the probability that the two samples compared come from the same population. In (b), which depicts a temporal change, the pre- and post-1989 samples are shown by solid and grey symbols, respectively. In all other panels, the spatially different volumes are marked by solid and grey symbols.

proposed that active magma chambers are surrounded by crustal volumes with increased *b* in their immediate vicinities.

The Mammoth Mountain area

The intrusion of 1989 has been documented in detail through seismic and geodetic observations (Hill *et al.* 1990; Hill 1996; Cramer & McNutt 1997). It is believed to have progressed from below to a depth of about 4–5 km. Our analysis of the FMD in the intrusion region is in agreement with this model. We detect a major *b*-value anomaly ($b > 1.6$) with a radius of 1 km below 7 km depth (Figs 3 and 4), which we interpret to indicate that a major magma body is located at this depth and below it in the aseismic crust. Straight above this major anomaly, at 5 km depth, at the centre of the seismicity, we find another, smaller anomaly ($r = 0.5$ km) of high *b* values ($b = 1.5$). This anomaly we interpret as the termination point of the 1989 intrusion. The fact that the anomaly at 5 km depth is clearly mapped, but that normal values separate the two anomalies, suggests that we cannot map relatively narrow cracks or conduits that may facilitate the transport of magma by our method. We reached the same conclusion in the Off-Ito intrusion: we were able to map the source of magma below 7 km depth clearly (Wyss *et al.* 1997), but not the path the magma took to the surface, which has been modelled independently from crustal deformations and changes of gravity (Shimazaki 1989; Tada & Hashimoto 1991). Therefore, we suggest that the termination of the 1989 Mammoth Mountain intrusion at 5 km depth did not fizzle out in a narrow crack, but ended in a sizeable volume of broken crust, possibly a small magma chamber.

Another small anomaly of high *b* values is located at 1.3 km depth (Figs 3 and 4b). This anomaly should correlate with the location of geothermal expressions at the surface, as such a shallow anomaly does at Montserrat (Power *et al.* 1998). Julian *et al.* (1998) show the existence of low *Vp* and low *Vp*/*Vs* anomalies at shallow depths (1–2 km) beneath Mammoth Mountain. These coincide with locations of CO_2

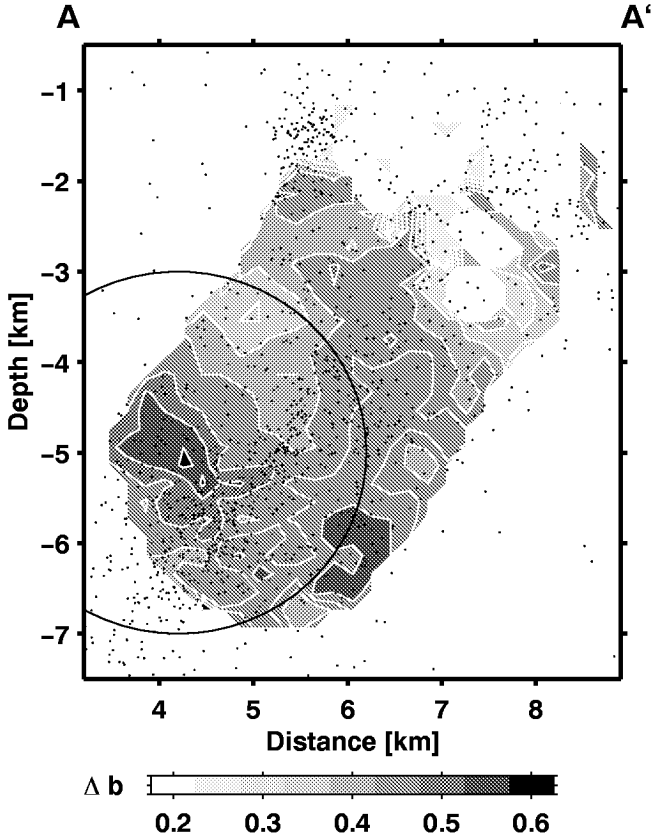

Figure 6. Differential *b*-value cross-section through the Mammoth Mountain area. Compared are the periods 1983–1989 and 1989–1990.5. Shown is the parameter $\Delta b = b_{(1989-91)} - b_{(1983-89)}$. A positive value indicates that the *b* value increased in the later period. The orientation of the cross-section is identical to that in Fig. 3(a) (A–A′) and marked in Fig. 1. Contours of Δb are spaced at 0.05 units. Only nodes where differences in the *b* value could be established at the 99 per cent confidence level are shaded grey.

gas release and tree kills at the surface. Note that the polarity of the *b*-value shift is consistent with these data; increasing fluid pressure lowers the effective stress and raises the *b* value.

We take the temporal increase of the *b* value around 1989.5 (Figs 2a and 6) as an indication that a drastic change in the crustal volume beneath Mammoth Mountain took place in 1989. Before the 1989 intrusion, we observe *b* values typical for tectonic crust. During and after the intrusion, the *b* values are much higher for most of the area under investigation, as shown by the differential *b*-value analysis (Figs 5b and 6). A similar progression of *b* values from $b = 0.8$ in the first of three major earthquake swarms during intrusions to $b = 1.3$ in the last one was observed at Off-Ito (Wyss *et al.* 1997). It is important to show by means of differential *b*-value mapping that the same crustal volume produces a different population of event sizes, because an overall shift in the *b*-value distribution can also be caused by a shift in activity from a low to a neighbouring high *b*-value volume.

The *b* value at Mammoth Mountain remains high until today, different from what is observed in tectonic aftershock sequences, where the *b* value returns to lower levels once the aftershock activity has decayed (Wiemer & Katsumata 1998). At Off-Ito volcano, Mount St Helens, and Mt Spurr, we observed that the frequency–magnitude distribution near the conduit itself (or dike in the case of Off-Ito) is not shifted towards high *b* values. We take this as an indication that these comparatively small features (tens of metres at most) that contain magma only for a short period do not permanently alter the surrounding rock in a volume large enough to be detected by our much larger ($r \approx 0.5$ km) sampling volumes. At Mammoth Mountain, on the other hand, the situation is different because, according to our interpretation, a substantial amount of magma or other fluid was permanently embedded into the crust at 4–5 km depth.

The interpretation that the increase of the *b* value in 1989 was due to a stress change is not plausible because we would have to assume that the intrusion was associated with a decrease of the ambient stress. Since all the evidence indicates the opposite (Langbein *et al.* 1993; Hill *et al.* 1990) we reject this interpretation in favour of proposing that the heterogeneity of the crust was increased through the introduction of new cracks by the stress exerted by the intrusion, or that the fluid pressure increased. If these newly created cracks are orientated in all directions, they will have a high fractal dimension *D*. If $D = 2b \approx 3$ (Turcotte 1992), then the volumes of high *b*-value anomalies are filled with cracks of all sizes and orientations. Under these conditions, the likelihood of large earthquakes occurring is decreased because a rupture terminates when it encounters an existing crack orientated unfavourably for failure. In such a highly fractured crust, we observe many small ruptures but few larger ones, which is what we see in the frequency–magnitude distribution. After the intrusion stops, this newly created system of cracks continues to produce earthquakes on these multiple faults. Healing of these cracks will probably take many years.

An alternative interpretation is that the latent heat introduced by the intrusion causes a change in the frequency–magnitude distribution towards higher *b* values. However, very little is known about this phenomenon, which is reported by one article on laboratory experiments only (Warren & Latham 1970). The interpretation that the anomalously high *b* values are due to greater heterogeneity (more cracks of all orientations) is the same in this hypothesis, only the cause would be assumed to be the temperature gradient rather than stress. The fact that we observe an almost instantaneous increase in *b* values (Fig. 2a) to distances of 2.5 km from the magma reservoir (Fig. 6) suggests that temperature differences could not be the agent bringing about these changes because the heat conductivity of crustal rocks is too low. Therefore, we prefer the hypothesis that the stress pulse due to the intrusion caused additional cracks in the crust surrounding the intrusion, or increased pore and gas pressure, leading to an increase in *b* values.

Seismicity south of the resurgent dome

The seismicity south of Long Valley Caldera shows an anomaly of high *b* values at the northernmost end of the seismicity, closest to the resurgent dome (Figs 7 and 8). Areas of high *b* value ($b > 1.5$) are quite limited in size, with the main anomaly occupying a volume with $r = 2.5$ km, approximately. For the rest of the tectonically active crust south of the immediate vicinity of the resurgent dome, the *b* values are generally below 1.0. In addition, *b* values in these 'normal' crustal volumes show a tendency to decrease with depth, which is in agreement

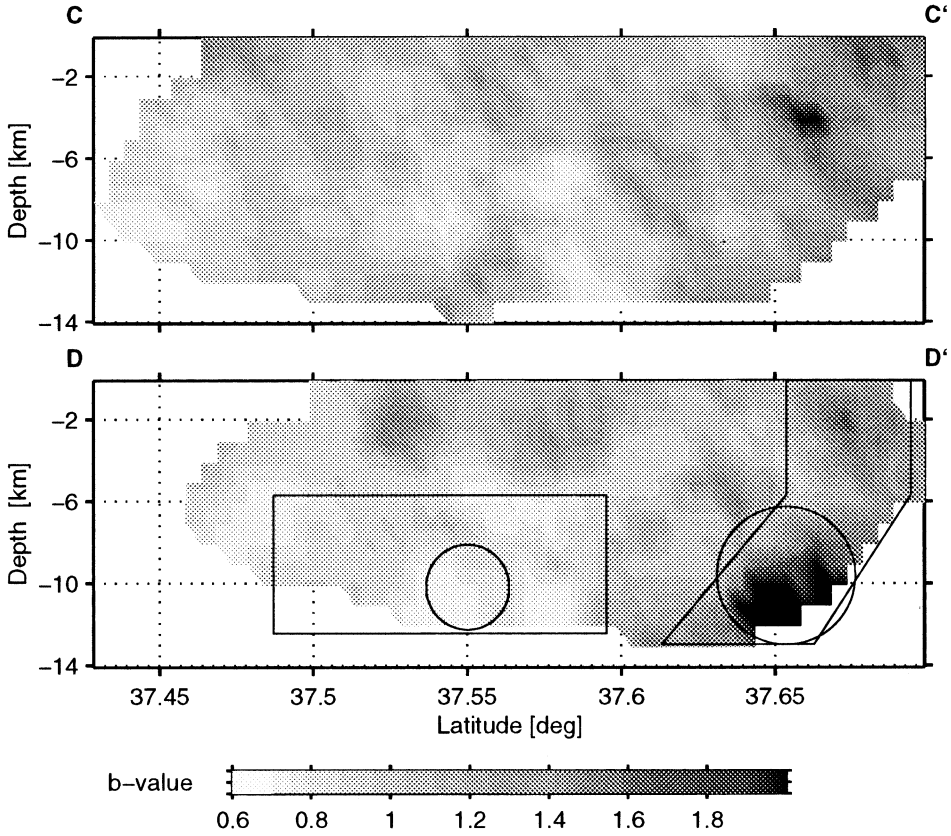

Figure 7. (a) North–south cross-sectional view of the *b* value along profile C–C′ in the Long Valley area (Fig. 1). The cross-section represents a vertical slice through the 3-D matrix of *b* values. High *b* values (dark) are concentrated on the northernmost edge of the cross-sections, near the resurgent dome. (b) North–south cross-sectional view of the *b* value along profile D–D′ (Fig. 1). Black circles and polygons indicate volumes compared in Figs 5(c) and (d).

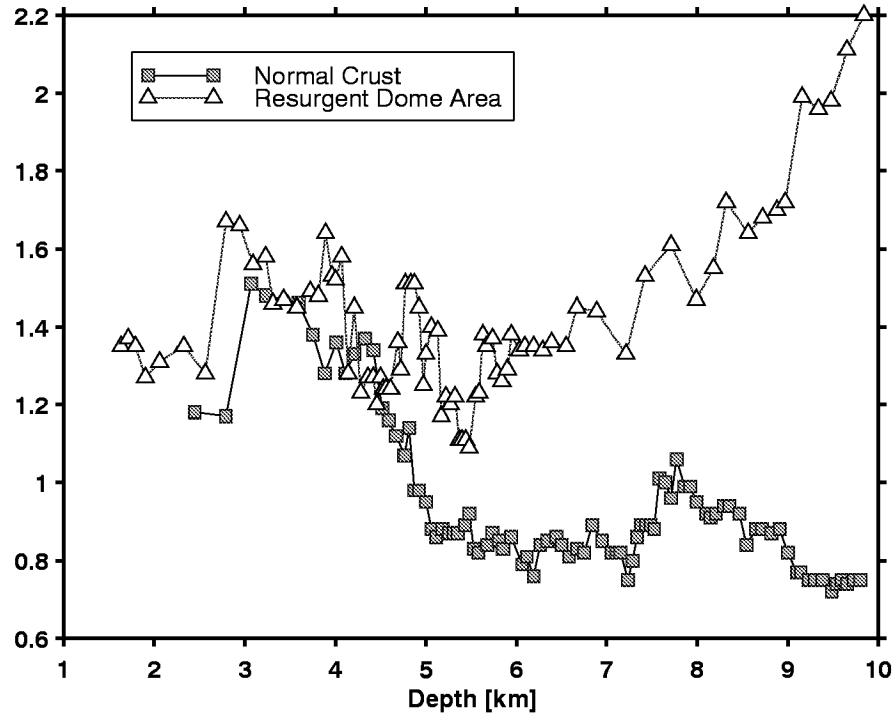

Figure 9. *b* value as a function of depth for the northernmost portion of the seismicity (white triangles), and the seismicity south of Long Valley in the Sierra Nevada (grey squares).

with observations for faults of the San Andreas system (Eaton *et al.* 1970; Wyss 1973; Mori & Abercrombie 1997; Wiemer & Wyss 1997) and is possibly caused by the increased stress at depth (Wyss 1973; Wiemer & Wyss 1997). However, the northernmost volume with anomalously high b values is also anomalous in that we observe an increase of b with depth rather than a decrease (Fig. 9). The difference in polarity of the b-gradient with depth indicates a fundamental difference between these crustal volumes and is consistent with the magma body centred at 11.5 km depth that has been proposed in other studies (e.g. Weiland *et al.* 1995).

The thickness of the high b-value rim that separates the aseismic crust to the north of the seismically active crust from the crust containing 'normal' b values in the south can be estimated to be 5 km or less (Figs 7 and 8). Since we observe anomalously high b values at essentially all depths along the northernmost part of the seismically active volume near the resurgent dome we must conclude that this crust is highly fractured at all depths.

Hill (1992) noted that the maximum depth of seismicity deepens from 4 km inside the caldera to 12 km in the Sierra Nevada to the south, and explained this feature as being caused by temperature-related changes in the brittle–plastic transition zone. The high b values in the northern portion of the seismicity, inside the caldera and adjacent to inferred magma bodies, are consistent with the interpretation of Hill. We propose that such a highly fractured crust could have been produced by multiple intrusions that have invaded this volume in the past. The intrusions were probably similar to the 1980–83 intrusions at this location, or the 1989 Mammoth Mountain intrusion. At shallow depth, hydrothermal activity and gas exsolution could also cause high b values.

These results obtained for Long Valley Caldera are in agreement with our earlier investigation of spatial variations of the b values at Mount St Helens (Wiemer & McNutt 1997) and at Off-Ito volcano (Wyss *et al.* 1997). In these studies we concluded that active magma bodies, and possibly the permanent alteration of the surrounding rock due to violent vesiculation and volatile exsolution, cause a significant increase in the b value in the surrounding area. The analysis of the seismicity in the Long Valley region supports our hypothesis that volcanic areas do not simply show a high b value, but contain pockets of high b value, which are distributed in otherwise normal crust.

The highest b values found ($b \approx 1.8$) are comparable to, or higher than, what we observed at Mount St Helens and Off-Ito volcano. b values greater than 1.5 are quite uncommon in the normal crust; however, they do occur in creeping segments of faults (Wiemer & Wyss 1997; Amelung & King 1997) and in aftershock zones (Wiemer & Katsumata 1998). High b-value volumes are therefore not unique to volcanic areas, although they are more common there.

Could the high b values result from a systematic error in the hypocentre locations or magnitude determination? If the location accuracy depends strongly on magnitude, artefacts can be introduced into the spatial b-value maps. Jolly (personal communication, 1997) has suggested that the shallow volume of high b values observed at Mt Spurr (Wiemer & McNutt 1997) might at least partially be caused by the systematic mislocation of larger events due to saturation of the analogue recording system for earthquakes with $M > 2$. We offer the following evidence that the described anomalies at Long Valley are real and not artefacts introduced by systematic mislocations or magnitude determination errors.

(1) There is no systematic dependence of the hypocentral error as reported by hypoellipse (Lahr 1989) on magnitude.

(2) The results remain the same if we use only a subset of earthquakes with RMS error < 0.1 s

(3) The network in the Long Valley region is quite dense (mean distance between stations is about 5 km), and an average of about 12 stations reported arrival times for each event.

(4) Differences in b value between the volumes are strong and are defined for several magnitude units.

(5) Differences can be defined for volumes containing many (> 1000) earthquakes.

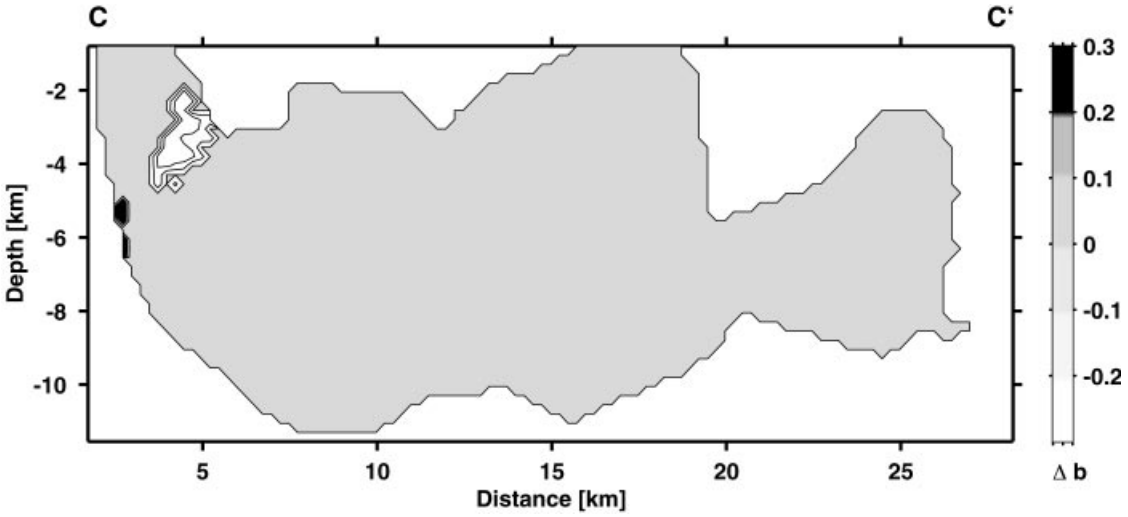

Figure 10. North–south cross-sectional view of the differential b value along profile C–C′ (Fig. 1). Compared are the periods 1989–1997.5 and 1997.5–1997.86. Shown is the parameter $\Delta b = b_{(1989-97.5)} - b_{(1997.5-197.86)}$. A positive value indicates that the b value increased in the later period. Contours of Δb are spaced at 0.1 units. Only nodes where differences in the b value could be established at the 99 per cent confidence level are shaded grey. Only two small volumes of significantly changed b value can be detected.

(6) Almost all frequency–magnitude distributions follow a Gutenberg–Richter type power law closely, without showing depletion or enrichment for certain magnitude bands. For the above reasons, we consider it unlikely that the high *b*-value regions are artefacts of systematic mislocations.

The 1997 activity

In June of 1997 the seismicity rate increased significantly in the volumes adjacent to the resurgent dome. This increase in activity coincides with a slight increase in deformation rate and has been interpreted as a small increase in pressure within the magmatic body at depth. Using the technique of differential *b*-value mapping we investigate whether a significant change in the *b* value occurred as a result of this pressure increase. In Fig. 10 we present a differential *b*-value map following profile C–C′ (Fig. 1). We sample volumes of 2 km radius and compare the periods 1994–1997.5 and 1997.5–1997.86. Nodes are only coloured if a change in *b* value was judged to be significant at the 99 per cent confidence level. We find only two areas of significantly changed *b* value, and the changes detected are generally small. No distinct volumes of increased *b* value similar to what we observe underneath Mammoth Mountain in 1989 (Fig. 6) can be identified. We interpret our analysis (Fig. 10) to be consistent with a small increase in stress due to an increase of pressure within the magma body at depth. This stress increase will cause more cracks to fail, causing an increase in seismicity rate. However, because the average crack distribution remains basically unaltered by a small increase in stress, earthquakes follow the same size distribution, and hence *b* value, as observed previously.

Capabilities and limitations of interpretations of *b*-value anomalies

Stress, material properties, temperature, or any combination of these parameters can modulate the frequency–magnitude distribution or the average crack size in the crust. Thus, *b*-value anomalies in different tectonic environments may be interpreted in different ways. However, the almost instantaneous increase of *b* values during an intrusion episode, documented above, cannot be explained by a stress increase (which should have lowered the *b* value) or a change of temperature gradient (which could not reach the volumes affected). Therefore, we are left with an increase of the heterogeneity through the introduction of new cracks, or an increase in pore pressure through the introduction of fluids, as the only reasonable interpretations. Based on these arguments and based on the observations at the other volcanic systems analysed to date (Mount St Helens, Mt Spurr, Off-Ito, and Long Valley) we conclude that the following statement may be true: in the vicinity of an active magma system the frequency–magnitude distribution is shifted towards high *b* values, due to greater crack density and exsolution of volatiles. This is not necessarily a surprising conclusion since a hot and gas-rich intruded body of magmatic material should be expected to make its presence know in the immediate surroundings.

Therefore, spatial mapping of the frequency–magnitude distribution can be used to assist in defining the locations of active magma bodies. For example, we suggest that from the analysis of the frequency–magnitude distribution in the Mammoth Mountain area (Figs 3 and 4) one can conclude that the main magma body is located below 8 km depth, and that the 1989 intrusion did not progress above 4–5 km depth. In the crust below the resurgent dome in the Long Valley area, the anomalously high *b* values at essentially all depths can be interpreted to indicate that multiple past intrusions into this volume have created a highly fractured crust (Figs 7 and 8).

CONCLUSIONS

Significant and extremely strong variations in the frequency–magnitude distribution as a function of both space and time can be detected in the Long Valley region.

The intrusion in 1989 underneath Mammoth Mountain caused a significant increase in the *b* value from $b \approx 0.8$ to $b \approx 1.4$. Until today, *b* values have not returned to the lower pre-intrusion values. Drastic changes as a function of time in the *b* value are rarely observed in non-volcanic regions and are an indication of a drastic change in the environmental conditions that control earthquake size distribution.

Distinct volumes of anomalously high *b* values can be clearly mapped underneath Mammoth Mountain. The highest *b* values ($b = 1.8$) are detected below 7-km depth in a volume with 1 km radius, a second anomalous volume ($r = 0.5$ km) occurs between 4 and 5 km depth at the centre of the seismic activity, and normal *b* values are found throughout the rest of the seismically active crust. This confirms the hypothesis that an intrusion of either water or magma advanced to about 4–5 km depth in 1989.

The *b* values are much higher ($b > 1.5$) closer to the resurgent dome in Long Valley than further to the south ($b < 1$). This supports the hypothesis that the magma located to the north of this seismically active volume permanently altered the frequency–magnitude distribution or average crack size in this area.

We propose that spatial mapping of the frequency–magnitude distribution can be used to aid in the identification of magma bodies since high *b* values near active magma bodies are a necessary (but not sufficient) condition.

ACKNOWLEDGMENTS

The authors would like to thank Cliff Frohlich, Rolf Schick and Hilary Fletcher for helpful comments and suggestions. We are grateful to the Northern California Earthquake Data Centre for proving the earthquake catalogues investigated and to David Hill and Chris Cramer for supplying information about Long Valley Caldera. This work was supported by the Wadati endowment of the Geophysical Institute of the University of Alaska Fairbanks, NSF grant EAR 9614783, and the Science and Technology Agency of Japan. A portion of this work was supported by the US Geological Survey as part of the Volcano Hazards and Geothermal Studies Program, and by additional funds from the State of Alaska through the Alaska Volcano Observatory (SM).

REFERENCES

Abercrombie, R.E., 1995. Earthquake source scaling relationships from −1 to 5 ML using seismograms recorded at 2.5-km depth, *J. geophys. Res.,* **100,** 24 014–24 036.

Abercrombie, R.E. & Brune, J.N., 1994. Evidence for a constant b-value above magnitude 0 in the southern San Andreas, San Jacinto, and San Miguel fault zones and at the Long Valley caldera, California, *Geophys. Res. Lett.,* **21,** 1647–1650.

Aki, K., 1965. Maximum likelihood estimate of b in the formula log N = a–bM and its confidence limits, *Bull. Earthq. Res. Inst., University of Tokyo,* **43,** 237–239.

Amelung, F. & King, G., 1997. Earthquake scaling laws for creeping and non-creeping faults, *Geophys. Res. Lett.,* **24,** 507–510.

Bailey, R.A. & Hill, D.P., 1990. Magmatic unrest at Long Valley caldera, California, 1980–90, *Geoscience Can.,* **17,** 175–178.

Cramer, C.H. & McNutt, S.R., 1997. Spectral analysis of earthquakes in the 1989 Mammoth Mountain swarm near Long Valley, California, *Bull. seism. Soc. Am.,* **87,** 1454–1462.

Dixon, T.H., Mao, A., Bursik, M., Heflin, M., Langbein, J., Stein, R. & Webb, F., 1997. Continuous monitoring of surface deformation at Long Valley Caldera, California, with GPS, *J. geophys. Res.,* **102,** 12 017–12 034.

Dvorak, J.J. & Dzurisin, D., 1997. Volcano geodesy: The search for magma reservoirs and the formation of eruptive vents, *Rev. Geophys.,* **35,** 343–384.

Eaton, J., O'Neil, M. & Murdock, J., 1970. Aftershocks of the 1966 Parkfield-Cholame, California, earthquake: a detailed study, *Bull. seism. Soc. Am.,* **60,** 1151–1197.

Gross, W.K. & Savage, J.C., 1987. Deformation associated with the 1986 Chalfant Valley earthquake, eastern California, *Bull. seism. Soc. Am.,* **77,** 306–310.

Gutenberg, R. & Richter, C.F., 1944. Frequency of earthquakes in California, *Bull. seism. Soc. Am.,* **34,** 185–188.

Habermann, R.E., 1987. Man-made changes of seismicity rates, *Bull. seism. Soc. Am.,* **77,** 141–159.

Habermann, R.E., 1991. Seismicity rate variations and systematic changes in magnitudes in teleseismic catalogs, *Tectonophysics,* **193,** 277–289.

Hamilton, R.M., 1967. Mean magnitude of an earthquake sequence, *Bull. seism. Soc. Am.,* **57,** 1115–1116.

Hill, D.P., Ellsworth, W.L., Johnston, M.S.J., Langbein, J.O., Oppenheimer, D.H., Pitt, A.M., Reasenberg, P.A., Sorey, M.L. & McNutt, S.R., 1990. The 1989 earthquake swarm beneath Mammoth Mountain, California: An initial look at the 4 May through 30 September activity, *Bull. seism. Soc. Am.,* **80,** 325–339.

Hill, D.P., 1992. Temperatures at the base of the seismogenic crust beneath Long Valley caldera, California, and the Phlegrean Fields caldera, Italy, in *Volcanic Seismology, IAVCEI Proc. in Volcanology 3,* pp. 432–461, eds Gasparini, P., Scarpa, R. & Aki, K., Springer Verlag, Berlin, Heidelberg.

Hill, D.P., 1996. Earthquakes and carbon dioxide beneath Mammoth Mountain, California, *Seism. Res. Lett.,* **67,** 8–15.

Hill, D.P., Johnston, M.J.S. & Langbein, J.O., 1995. Response of Long Valley caldera to the Mw = 7.3 Landers, California, earthquake, *J. geophys. Res.,* **100,** 12 985–13 005.

Ishimoto, M. & Iida, K., 1939. Observations of earthquakes registered with the microseismograph constructed recently, *Bull. Earthq. Res. Inst., University of Tokyo,* **17,** 443–478.

Julian, B.R., Pitt, A.M. & Foulger, G.R., 1998. Seismic image of a CO_2 reservoir beneath an active volcano, *Geophys. J. Int.,* **133,** F7–F10.

Lahr, J.C., 1989. HYPOELLIPSE/version 2.00: A computer program for determining local earthquakes hypocentral parameters, magnitude, and first motion pattern.

Langbein, J., Hill, D.P, Parker, T.N. & Wilkinson, S.K., 1993. An episode of reinflation of the Long Valley Caldera, eastern California: 1989–91, *J. geophys. Res.,* **98,** 15 851–15 870.

Miller, C.D., 1985. Holocene eruptions at the Inyo volcanic chain, California—implications for possible eruptions in the Long Valley caldera, *Geology,* **13,** 14–17.

Mogi, K., 1962. Magnitude–frequency relation for elastic shocks accompanying fractures of various materials and some related problems in earthquakes, *Bull. Earthq. Res. Inst., University of Tokyo,* **40,** 831–853.

Mori, J. & Abercrombie, R.E., 1997. Depth dependence of earthquake frequency–magnitude distributions in California: Implications for the rupture initiation, *J. geophys. Res.,* **102,** 15 081–15 090.

Ogata, Y., Imoto, M. & Katsura, K., 1991. 3-D spatial variation of b-values of magnitude–frequency distribution beneath the Kanto district, Japan, *Geophys. J. Int.,* **104,** 135–146.

Pitt, A.M. & Hill, D.P., 1994. Long-period earthquakes in the Long Valley caldera region, eastern California, *Geophys. Res. Lett.,* **21,** 1679–1682.

Power, J.A., Wyss, M. & Latchman, J.L., 1998. Spatial variations in frequency–magnitude distribution of earthquakes at Soufriere Hills volcano, Montserrat, West Indies, *Geophys. Res. Lett.,* **25,** in press.

Rundle, J.B. *et al.,* 1986. Deep drilling to the magmatic environment in Long Valley caldera, *EOS, Trans. Am. geophys. Un.,* **67,** 490–491.

Rundle, J.B. & Whitcomb, J.H., 1984. A model for deformation in Long Valley, California, 1980–83, *US geol. Survey Open-file rep.* **84–939,** 584–616.

Shi, Y. & Bolt, B.A., 1982. The standard error of the Magnitude-frequency b value, *Bull. seism. Soc. Am.* **72,** 1677–1687.

Shih, X.R. & Meyer, R.P., 1990. Observation of shear wave splitting from natural events: South moat of Long Valley caldera, California, June 29 to August 12, 1982, *J. geophys. Res.* **95,** 11179–11195.

Shimazaki, K., 1989. Tectonics of dike injections off the eastern Izu Peninsula, in *Volcanoes and Plate Tectonics*, pp. 252–256, ed. Nakamura, K., University of Tokyo Press, Tokyo.

Scholz, C.H., 1968. The frequency–magnitude relation of microfracturing in rock and its relation to earthquakes, *Bull. seism. Soc. Am.*, **58,** 399–415.

Sieh, K. & Bursik, M., 1986. Most recent eruption of the Mono Craters, eastern central California, *J. geophys. Res.*, **91,** 12 539–12 571.

Sorey, M.L. *et al.,* 1993. Helium isotope and gas discharge variations associated with crustal unrest in Long Valley Caldera, California, 1989–92, *J. geophys. Res.* **98,** 15871–15889.

Tada, T. & Hashimoto, M., 1991. Anomalous crustal deformation in the northeastern Izu Peninsula and its tectonic significance—tension crack model, *J. Phys. Earth,* **39,** 197–218.

Turcotte, D.L., 1992. *Fractals and Chaos in Geology and Geophysics*. Cambridge University Press, Cambridge.

Urbancic, T.I., Trifu, C.I., Long, J.M & Toung, R.P., 1992. Space–time correlations of *b*-values with stress release, *Pageoph,* **139,** 449–462.

Utsu, T, 1965. A method for determining the value of b in a formula log n = a–bM showing the magnitude frequency for earthquakes, *Geophys. Bull. Hokkaido Univ.* **13,** 99–103.

Utsu, T., 1992. *On Seismicity*, Rpt Jt Res. Inst. Stat. Math., pp. 139–157, Inst. Stat. Math., Tokyo.

Warren, N.W. & Latham, G.V., 1970. An Experimental Study of Thermally Induced Microfracturing and its Relation to Volcanic Seismicity, *J. geophys. Res.*, **75,** 4455–4464.

Weiland, C.M. *et al.,* 1995. Nonlinear teleseismic tomography at Long Valley caldera, using three-dimensional minimum travel time ray tracing, *J. geophys. Res.*, **100,** 20 379–20 390.

Wiemer, S. & Benoit, J., 1996. Mapping the b-value anomaly at 100 km depth in the Alaska and New Zealand subduction zones, *Geophys. Res. Lett.*, **23,** 1557–1560.

Wiemer, S. & Katsumata, K., 1998. Spatial variability of seismicity parameters in aftershock zones, *J. geophys. Res.,* **88,** submitted.

Wiemer, S. & McNutt, S., 1997. Variations in frequency-magnitude distribution with depth in two volcanic areas: Mount St. Helens, Washington, and Mt. Spurr, Alaska, *Geophys. Res. Lett.* **24,** 189–192.

Wiemer, S. & Wyss, M., 1997. Mapping the frequency-magnitude distribution in asperities: An improved technique to calculate recurrence times, *J. geophys. Res.*, **102,** 15 115–15 128.

Wyss, M., 1973. Towards a physical understanding of the earthquake frequency distribution, *Geophys. J. R astr. Soc.*, **31,** 341–359.

Wyss, M., 1991. Reporting history of the central Aleutians Seismograph network and the quiescence preceding the 1986 Andreanof Island earthquake, *Bull. seism. Soc. Am.*, **81,** 1231–1254.

Wyss, M., Shimazaki, K. & Wiemer, S., 1997. Mapping active magma chambers by b-value beneath Off-Izu volcano, Japan, *J. geophys. Res.*, **102,** 20 413–20 433.

Zuniga, R. & Wyss, M., 1995. Inadvertent changes in magnitude reported in earthquake catalogs: Influence on b-value estimates, *Bull. seism. Soc. Am.*, **85,** 1858–1866.